THE ASTROPHYSICAL JOURNAL, 284:637–642, 1984 September 15

FAR-INFRARED AND SUBMILLIMETER OBSERVATIONS OF THE MULTIPLE CORES IN S255, W3, AND OMC-1: EVIDENCE FOR FRAGMENTATION?

D. T. JAFFE,[1, 2, 3] J. A. DAVIDSON,[2, 3, 4] M. DRAGOVAN,[2, 4] AND R. H. HILDEBRAND[2, 4, 5]

Received 1983 December 15; accepted 1984 March 15

ABSTRACT

We present far-IR and sub-mm maps of S255 which reveal the presence of a previously undiscovered cloud core 1′ north of S255-IR. This second core has a mass greater than the core in S255-IR (500 $M_\odot$ vs. 350 $M_\odot$) and a temperature $\sim$10 K lower (35 K vs. 45 K). We also present 40 μm–400 μm photometry of these two cores and of the previously observed double cloud cores in W3 and OMC-1 and use the mapping and photometry results to derive temperatures, densities, masses, and visual extinctions for the cores. The observations lead to several general conclusions about massive cloud cores and the young stars within them.

1. In all cases, the cores are associated with the youngest objects in more complex regions: very compact H II regions, H_2O maser centers, or 300–600 K near-IR sources. The young objects are coincident with the sub-mm peaks, indicating that they have formed within the cores rather than at their edges.

2. The cooler cores are probably not a new class of source but rather similar in mass and structure to the warmer cores but containing less luminous young stars.

3. Molecular line observations indicate velocity differences of 1.4–4 km s^{-1} between the two cores in a given cloud. If this difference is a result of rotation, the masses derived from the sub-mm fluxes and by assuming dynamical equilibrium are roughly comparable. If the multiple cores at different velocities result from large-scale fragmentation of a rotating parent cloud, approximately 90% of the initial angular momentum is now in the orbital motion of the cores. This reduction in angular momentum could have enabled the centers of the cores to continue their collapse to form the massive young stars that now heat them.

Subject headings: infrared: sources — interstellar: molecules — nebulae: H II regions — stars: formation

I. INTRODUCTION

The standard pictures of OB star formation in giant molecular clouds have the massive stars forming either at the edges or at the cores of 10^4–10^5 $M_\odot$ giant molecular clouds. Recent sub-mm measurements have shown that many massive stars in their earliest phases lie at the centers of very dense ($n_{H_2} \sim 10^5$–10^6 cm^{-3}) molecular cores of 10^2–10^3 $M_\odot$ within the larger clouds (Keene, Hildebrand, and Whitcomb 1982; Gezari 1982; Jaffe *et al.* 1983, 1984). Many cloud centers contain more than one core with typical separations of $\sim 10^{18}$ cm. In almost all cases, the cooler cores were not clearly visible in earlier molecular line or far-IR mapping of the regions. High resolution (3″) NH_3 observations with the VLA indicate that these cores in turn are clumpy on small scales (see, e.g., Genzel *et al.* 1982).

The cores of clouds where massive stars have recently formed have higher temperatures and densities than other portions of the clouds. In cases where several cores have formed stars in a small region and temperature and density both fall away from the excitation sources, molecular rotation line studies tend to smear the sources together. Optically thin submillimeter dust emission provides better contrast between the individual sources than molecular line observations and estimates of column density comparable in reliability to estimates derived from molecular line studies (Jaffe *et al.* 1984). Far-IR observations allow us to estimate the luminosities of the newly formed exciting stars as well as to detemine the dust temperatures in the cores.

We present here maps of the two cores in the S255 cloud at 60 μm, 100 μm, 185 μm, and 400 μm, as well as 40 μm–400 μm photometry of the S255 cores and of the cores in OMC-1 and W3 which we had mapped previously at 400 μm (Keene, Hildebrand, and Whitcomb 1982; Jaffe *et al.* 1983). We can use these observations to derive the physical parameters of the dense cloud cores. We can study the dynamics of the dense inner regions of giant clouds using the masses derived from the submillimeter data and kinematic information from molecular line observations.

II. OBSERVATIONS

We made the 40 μm–185 μm photometric observations of W3, OMC-1, and S255 and the 60 μm, 100 μm, and 185 μm maps of S255 in 1983 January on the 0.91 m telescope of the Kuiper Airborne Observatory with the Yerkes Observatory G-2 and H-1 photometers (Harper *et al.* 1984). For the photometry with the G-2 system, we used a 49″ aperture and three filters: sapphire and KRS6 ($\lambda_{eff} \sim 40$ μm), sapphire, CaF_2, and KRS5 ($\lambda_{eff} \sim 60$ μm), and a metal mesh bandpass interference filter with ($\lambda_{eff} \sim 100$ μm). The H-1 system had a measured beamsize of 50″. With this system, we used metal mesh interference filters with effective wavelengths of 135 μm, 160 μm, and 185 μm. The photometric measurements were made toward the positions listed in Table 1. We calibrated the fluxes relative to W3(OH) (Harper, private communication) using the iterative scheme described by Jaffe *et al.* (1984). The overall uncertainty in the absolute flux densities is about 30%.

[1] Space Sciences Laboratory, University of California, Berkeley.
[2] Enrico Fermi Institute, University of Chicago.
[3] Visiting Astronomer at the Infrared Telescope Facility which is operated by the University of Hawaii under contract from the National Aeronautics and Space Administration.
[4] Department of Physics, University of Chicago.
[5] Department of Astronomy and Astrophysics, University of Chicago.

For the 60 μm and 100 μm maps of S255, we used three of the seven spatial channels in the G-2 photometer with 33″ beams spaced by 55″. The observations were on a 15.″7 grid oriented in elevation and cross-elevation (7°–20° from NS–EW). The relative positions of the points are accurate to $\pm 5''$ and the absolute positions are good to $\pm 12''$. For the 185 μm map, we used the single channel H-1 system with a 50″ beam and mapped the source on a 19.″6 grid. For both the maps and the photometry, the telescope secondary switched at 27 Hz between two positions separated by 5′ in cross-elevation on the sky.

We made the sub-mm observations of S255 in 1982 November with the University of Chicago–NASA Ames ^{3}He cooled submillimeter photometer on the 3 m NASA infrared telescope on Mauna Kea. The system had a 50″ beamsize (full width to half-maximum) and a spectral response determined by a metal-mesh interference filter and the atmosphere with half-power points at 330 μm and 370 μm. The effective wavelength for the atmospheric conditions at the time of these observations was 350 μm. We have referred all fluxes to 400 μm assuming $S_\nu \propto \nu^{3.5}$. The chopper throw for these observations was 4′ East–West.

The 400 μm observations of OMC-1 and W3 were made under various atmospheric conditions in 1981 March and November and in 1982 November with the University of Chicago submillimeter photometer (Whitcomb, Hildebrand, and Keene 1980). The beam was approximately Gaussian with a full width of half-maximum of 48″. We calibrated the fluxes by observing Mars (in the case of OMC-1) and OMC-1 (in the case of W3) using the brightness temperature of Wright and Odenwald (1981). The OMC-1 value is a result of 10 independent measurements and the W3 IRS 5 value results from five measurements. The 400 μm fluxes of OMC-1 S and W3 IRS 4 were measured with respect to these two sources. Overall flux errors are approximately $\pm 25\%$.

III. RESULTS

Figure 1 shows maps of S255 at 60 μm and 100 μm (33″ resolution) and at 185 μm and 400 μm (50″ resolution). Superposed on the 400 μm map are the positions of the near-infrared sources S255–IRS 1 and IRS 2 (Pipher and Soifer 1976; Beichman, Becklin and Wynn-Williams 1979) the H_2O maser source (Lo and Burke 1973; Genzel and Downes 1977) and one compact and one weak, slightly extended H II region (Israel 1976; Beichman, Becklin, and Wynn-Williams 1979). The most remarkable feature in the 400 μm intensity distribution, which effectively traces H_2 column density (Hildebrand 1983), is the presence of two mass concentrations separated by 1′ (2×10^{18} cm at 2.5 kpc; Evans, Blair, and Beckwith 1977). The maps in Figure 1 show steady change from a single dominant source coincident with the H_2O/near-IR source in the south at 60 μm to two equally strong sources at 400 μm. This is also clearly reflected in the photometry in Figure 2 which presents 49″ beam 40 μm–400 μm spectra toward the two 400 μm peaks in S255. At 40 μm, the southern peak is 7 times stronger than the northern peak. The two peaks are equal in strength at 400 μm (see also Table 1). The 60 μm–100 μm color temperatures of these two peaks differ by 10 K (35 K in the north versus 45 K in the south).

The 400 μm continuum maps of OMC-1 (Keene, Hildebrand, and Whitcomb 1982) and W3 (Jaffe *et al.* 1983) also showed two similar-sized mass condensations in each source. Figure 2 presents 49″ beam 40 μm–400 μm photometry toward these cores as well. The W3 spectra use 30 μm–100 μm points from the 30″ resolution observations of Werner *et al.* (1980). Table 1 summarizes results derived from the spectra in Figure 2. These results imply that, as in S255, the two cores in both W3 and OMC-1 have considerably different temperatures (see also the previous $\lambda \leq 100$ μm data of Werner *et al.* (1976, 1980)). The luminosities of the more luminous core in each source are comparable. These hotter cores have luminosities 3–5 times the luminosities of the nearby cooler cores.

Table 2 presents a comparison of the parameters of W3, OMC-1, and S255 derived from the 400 μm maps and from the sub-mm fluxes given in Table 1. The beam averaged optical depths imply H_2 column densities of $0.4\text{–}3.2 \times 10^{23}$ cm^{-2} (Hildebrand 1983). The derived sizes of the individual components are all $\sim 3 \times 10^{17}$ cm, and the masses within 48″ of each 400 μm peak are $\sim 300\ M_\odot$. The peak H_2 density and A_v are derived assuming Gaussian density profiles for the sources (see Jaffe *et al.* 1983).

IV. DISCUSSION

a) *The Two Cores of S255-IR*

The near-infrared source S255–IR (Pipher and Soifer 1976) lies in between two optical/radio H II regions, S255 and S257,

TABLE 1

FAR-IR/SUBMILLIMETER SPECTRUM RESULTS

Object	Photometry Position (1950)	Distance (kpc)	Flux Density in 49″ Beam 40 μm	Flux Density in 49″ Beam 400 μm	$T_{60\,\mu m/100\,\mu m}$ [$\nu B_\nu(T)$]	$L_{40\,\mu m–400\,\mu m}$ ($10^4\ L_\odot$)
W3 IRS 4	02^{h}21^{m}43^{s}6 +61°52′49″	2.0	1400[a]	500	38	4.5
W3 IRS 5	02 21 53.0 +61 52 21	2.0	8000[a]	500	51	11
OMC-1 S	05 32 45.6 −05 25 25	0.5	15800	1700	47	1.0
OMC-1	05 32 46.6 −05 24 25	0.5	141000	2700	76	5.6
S255	06 09 58.2 +18 00 14	2.5	1430	200	45	2.6
S255 N	06 09 58.2 +18 01 14	2.5	220	210	35	0.9

[a] Flux density at 50 μm in a 30″ beam (Werner *et al.* 1980).

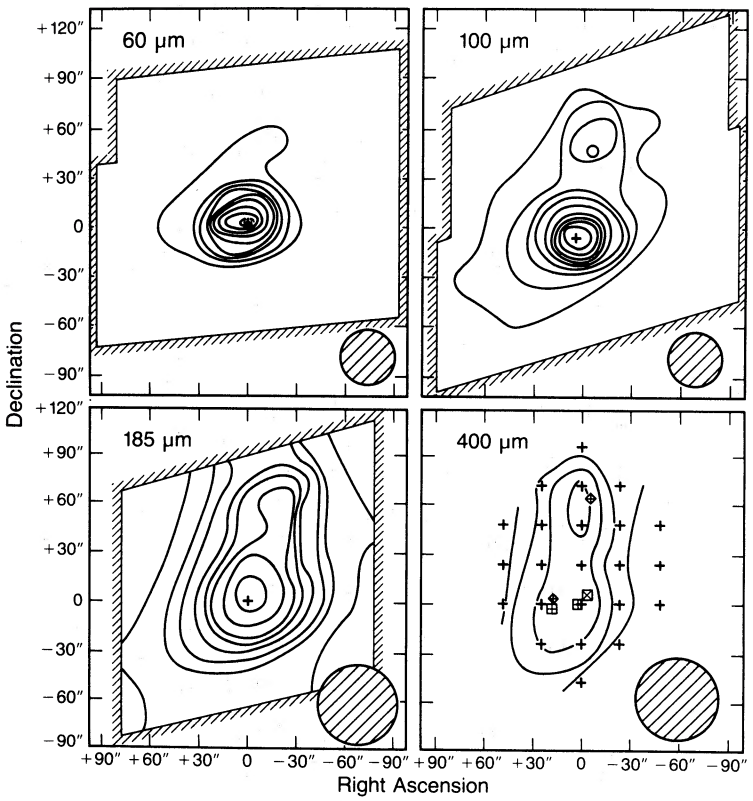

FIG. 1.—Far-IR and Sub-mm Maps of S225. For each map, the right ascension and declination are given as offsets from $06^h09^m58^s.5$, +18°00′12″ (1950). The hatched circle in the lower right corner of each map shows the half-power size of the beam. For the 60 μm, 100 μm, and 185 μm maps, the solid lines with exterior ticking denote the boundaries of the fully sampled area. The crosses give the position of maximum flux. The contours are at intervals of 10% of this flux beginning at 10% for the 60 μm and 100 μm maps and at 20% for the 185 μm map. The small crosses in the 400 μm map represent the points where the data were taken. The contours represent 30%, 50%, 70%, and 90% of the flux measured at the 0,0 position. The remaining symbols show the positions and positional uncertainties and various other objects. The small boxes with upright crosses show the near-IR sources IRS 1 and IRS 2 (Beichman, Becklin, and Wynn-Williams 1979), the diamonds show the compact H II regions (Israel 1976), and the box with the diagonal cross shows the H_2O maser center (Genzel and Downes 1977).

in the direction of the galactic anticenter. The radio, infrared, and maser sources near S255 make up the most compact and most obscured part of a ~10 pc long complex of ionized regions powered by late O and early B stars or by OB clusters (Israel 1976). The infrared and maser sources lie at the center of a ~30′ long CO cloud that extends behind the H II regions S255 and S257 (Evans, Blair, and Beckwith 1977). Our submillimeter observations (Fig. 1*d*) show that the cloud has two 300–500 $M_\odot$ cores: S255–IR and S255 N. The two near-IR sources in the southern core (S255–IR) may imply the presence of a cluster of luminous pre-main-sequence stars (Beichman, Becklin, and Wynn-Williams 1979). This core has a 40 μm–400 μm luminosity of $2.6 \times 10^4\ L_\odot$ within a 25″ radius. The 2 μm–20 μm luminosity is ~10% of this value (Pipher and Soifer 1976). The northern core has a luminosity of only $1 \times 10^4\ L_\odot$. There are no sensitive near-IR data on the region near this core. If the compact radio source of 192.58–0.04 (Fig. 1*d*; Israel 1976) is deeply embedded in this core, it may produce all of the observed far-IR luminosity. The observed optically thin radio flux implies 1.6×10^{46} ionizing photons are absorbed by the gas each second. This ionization rate requires a single ZAMS B0.5 star with a luminosity of $10^4\ L_\odot$ (Panagia 1973).

The peak molecular hydrogen densities we have derived from the submillimeter observations ($0.5–2.5 \times 10^5$ cm^{-3}, Table 2) agree well with the values inferred from rotational transitions of H_2CO but are a factor of 20–100 higher than the

TABLE 2

SUBMILLIMETER RESULTS

Object	$\tau_{400\ \mu m}$ (48″ beam)	400 μm Size (10^{17} cm)	Peak H_2 Density (10^5 cm^{-3})	Peak A_v	Mass in 48″ Beam ($M_\odot$)
W3 IRS 4	0.021	15[a]	1.5	250	650
W3 IRS 5	0.014	9[a]	3.0	300	450
OMC-1 S	0.053	2.9[b]	30.0	800	100
OMC-1	0.044	2.6[b]	30.0	750	100
S255	0.007	21	0.5	70	350
S255 N	0.010	10	2.5	250	500

[a] Jaffe *et al.* 1983.

[b] Keene, Hildebrand, and Whitcomb 1982.

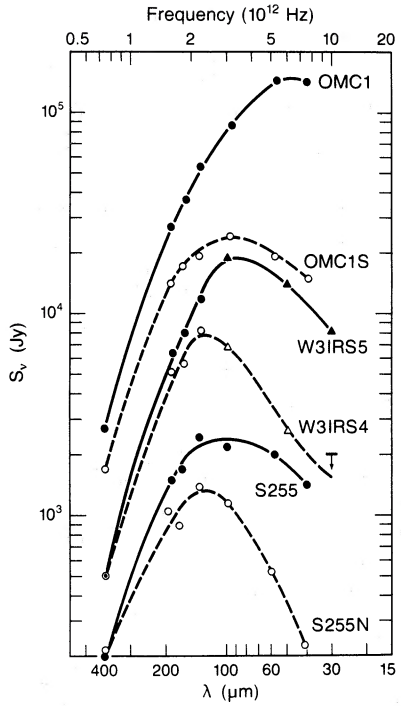

FIG. 2.—40 μm–400 μm Spectra of the Cores. The filled and open circles show data from the present work taken with a 48″ beam. The filled and open triangles are 30″ beam flux densities from the work of Werner *et al.* (1980). The lines connecting the points were inserted as an aid to the eye and do not represent fits to the data. The positions for the photometry are listed in Table 1.

value derived from ^{13}CO column density and ^{12}CO sizes (Evans, Blair, and Beckwith 1977). The lower values from the CO observations result partly from using the optically thick $^{12}C^{16}O$ line to measure the cloud size. (The half-power size of the temperature distribution derived from the ^{12}CO is 5–10 times larger than the half-power size of the density distribution derived from the sub-mm continuum.) The derivation of *peak* density (assuming a Gaussian density profile) from the sub-mm results (Table 2) and *beam averaged* density from the ^{13}CO results causes a factor of two difference in the numbers from the two techniques. The remaining difference may result in part from an optical depth in the ^{13}CO line greater than one, since the H_2 column densities inferred from the ^{13}CO optical depth and the $^{13}CO/H_2$ ratio of Dickman (1978) are about a factor of 5 less than the H_2 column densities derived from the sub-millimeter observations.

The luminosities and masses of the two cores in S255 are comparable to the same quantities in W3 and OMC-1. The lower peak H_2 densities and optical depths in the cores of S255 and W3 than in the OMC-1 cores (Table 2) could be a result of beam dilution at the greater distances to these sources and of a non-Gaussian density distribution (see Jaffe *et al.* 1983). What is remarkable in S255, as in the other two sources, is the strong concentration of mass around young objects: in this case, a near-IR cluster and a compact H II region.

In all three sources, the sub-mm results give strong evidence that the young objects are deeply embedded in the cloud cores rather than lying at the edges of the cores. Projection effects cannot account for the good positional coincidence of sub-mm peaks with H_2O masers or compact H II regions in so many cases. Jaffe *et al.* (1984) obtain a similar result for luminous young sources near M17. The central location of the young objects combined with the existence of multiple cores leads to a plausible alternative explanation to the usual "blister" picture of compact H II regions: Massive molecular clouds could break up into a number of 10^2–10^3 $M_\odot$ cores all of which form stars. The cores containing O stars then would be destroyed rapidly, leaving H II regions next to dense molecular cores containing early B stars. These latter cores would then appear as hotspots in molecular line maps but could have dust column densities that would make it impossible for all but the most sensitive near-infrared surveys to locate their internal heat sources.

b) The Nature of Cloud Cores

Closely grouped (separation $\sim 10^{18}$ cm), massive ($M \sim 10^{2.5}$ $M_\odot$) cloud cores are probably very common in regions where massive stars are forming or have recently formed. Sub-millimeter observations have shown such multiple cores to exist in at least two clouds not discussed in the present work: NGC 6334I (Cheung *et al.* 1978; Gezari 1982) and OMC-2 (Whitcomb *et al.* 1984). Examples of single, isolated cores also exist (e.g., 12.4 + 0.5, Jaffe *et al.* 1984; W3(OH) and W75 N; Jaffe, unpublished) but all of these cores are in larger clouds containing other star-forming regions. Evidence of multiple cores from molecular line mapping is inconclusive since the commonly used $^{12}C^{16}O$ and $^{13}C^{16}O$ $J = 1$–0 transitions are both optically thick in the inner regions of molecular clouds. Small-scale structure is often hard to pick out in these lines since they can be excited at low densities and one therefore sees the envelope of the cloud as well as the core. In addition, nearby peaks may be smeared together even when one uses optically thin rotational lines because of the effects of temperature gradients on the column densities in a given state (Jaffe *et al.* 1984). We can use our far-IR and sub-mm results together with previously published radio and infrared data to understand the nature of the cores and their luminosity sources.

i) *Temperature, Structure, and Luminosity*

There is no evidence that the exciting stars in the cooler cores in the three clouds studies here are different in any fundamental respect from the stars in the warmer cores. The cores have temperatures typical of far-IR sources in their luminosity range. Two of the three are known to contain compact H II regions. It is therefore likely that they do not represent a new type of object but merely demonstrate the presence of previously difficult to observe cores near other cores with slightly higher temperatures.

Observed dust temperatures in molecular clouds depend on the radial distribution of dust, the luminosity of the exciting stars, and the physical extent of the beam used for the observations. There are no significant correlations between the temperatures and luminosities of all the cores in the three clouds we observed. Tables 1 and 2 *do* show a correlation of luminosity with temperature between the two cores in a given source, however, that is consistent with a model in which the density structure in the two cores is similar and only the luminosity differs. The dust distribution rather than the linear beam size probably plays a dominant role in scattering the source to source temperature-luminosity relation. Sources with luminosities $\sim 10^4$ times less than the OMC-1 cores and 3 times closer have temperatures only 2 times smaller (Davidson and Jaffe 1984) instead of the factor of more than 6 one would expect from sources with similar structures.

ii) *Cloud Cores and Clusters*

There is clear evidence that some of the cloud cores contain young clusters rather than single stars. The near-IR results provide such evidence for OMC-1 (cf. Downes *et al.* 1981), W3 IRS 5 (Howell, McCarthy, and Low 1981; Wynn-Williams, Becklin, and Neugebauer 1972) and in S255–IR (Beichman, Becklin, and Wynn-Williams), if we believe that S255 IRS 2 has its own exciting star. There is also indirect evidence that W3 IRS 4 has more than one exciting star (Jaffe *et al.* 1983). Observational limitations prevent us from knowing if the cores contain only a small group of stars of roughly equal mass or entire clusters extending to much lower masses. The small groups would have total stellar masses of 1–5% of the core masses. Clusters could have masses much closer to the mass of the interstellar material.

iii) *Relationship of Cloud Cores to Surrounding Regions*

All three of the sources studied here lie near bright *optical* H II regions: W3 near IC 1795, OMC-1 near the Orion nebula, and S255–IR near S255. This is purely a selection effect. While no unbiased sample of compact cores exists, it is clear that many cores exist in regions containing neither optical nor radio H II regions of any size or strength (Jaffe *et al.* 1984). The 10^2–10^3 $M_\odot$ molecular cloud cores in the present three sources, as well as the cores in OMC-2 and NGC 6334, are embedded in more extensive giant molecular clouds and strings of H II regions in various stages of development. All of the sources except S255 have axes between their cores roughly parallel to the long dimension of the larger cloud. The line joining S255 and S255 N is roughly perpendicular to the general orientation of its parent cloud.

iv) *Clumping and Extinction*

The peak visual extinctions, A_v, derived from sub-mm observations and listed in Table 2 range from 70 to 800 magnitudes. As is the case for the peak densities, the extinctions in the more distant objects could be considerably higher than the values in Table 2. The clumpy distribution of gas on 1″–5″ scales shown by the VLA maps of NH_3 in OMC-1 and other sources (see, e.g., Genzel *et al.* 1982; Ho, Genzel, and Das 1982) indicate that the 10^2–10^3 $M_\odot$ cores observed in the sub-mm have smaller scale condensations within them. Since $\tau > 1$ for many of the NH_3 emission lines and since the abundance of NH_3 is so uncertain, it is difficult to estimate the masses of these smaller clumps. In OMC-1, the observability of 10 μm–20 μm sources despite the large amount of overlying cold dust results from the clumpy distribution of the extincting dust in the core (Wynn-Williams *et al.* 1984). In general, the large extinctions result in weak 20 μm sources and very weak 3 μm–10 μm sources in dense cloud cores. It may be necessary, therefore, to use techniques other than near-IR observations to find newly formed or forming stars in the cloud cores. High resolution submillimeter observations (10″ with the new generation 10 m telescopes) and multi-transition NH_3 observations with the VLA, while they cannot provide direct information about the protostars, may provide us with information about the temperatures and densities in the regions immediately surrounding them.

v) *Finding Multiple Cores*

The observations of closely spaced multiple cloud cores at 400 μm and at shorter wavelengths point up several difficulties in finding new examples of multiple cores in 60 μm and 100 μm *IRAS* survey data. In the sources we are studying here, the cloud cores of roughly equal mass lie only $\sim$60″ apart. In all cases, one core is 3–5 times brighter at 60 μm and 2–4 times brighter at 100 μm. Confusion may make it hard to draw any strong inferences about the numbers and natures of multiple cores in other regions from *IRAS* survey data. One possible telltale could be a shift in the peak position as a function of wavelength in a source that is extended in one direction but unresolved in another. A better discovery method would be to survey a limited sample of far-IR sources at 400 μm.

c) Cloud Cores and Fragmentation

All three of the clouds in the present study have velocity shifts between the two massive cores. In W3, the shift is $\sim$4 km s^{-1} (Brackmann and Scoville 1980), in OMC-1, it is $\sim$1.4 km s^{-1} (Ziurys *et al.* 1981), and in S255, it is $\sim$1.7 km s^{-1} (Ho, Martin, and Barrett 1981). The masses derived from assuming that the velocity shifts represent rotation and those derived from the sub-mm flux measurements (see Jaffe *et al.* 1983) are comparable, differing by 20% for W3 and by factors of 6 and 3 for OMC-1 and S255, respectively. Although the velocity shifts do not *necessarily* reflect motion in bound orbits (the orbital time scales of $\sim 10^5$ years are nearly as long as the usual estimates for compact H II region and H_2O maser center lifetimes of a few 10^5 years), it is interesting to consider the effect the collapse of a single rotating cloud into two separate cores would have on the ease with which less massive condensations could form stars.

The principal effect of fragmentation on large scales is to transfer angular momentum from cloud rotation to orbital motion of the massive fragments. Consider a cloud with total angular momentum J_T which breaks up into two identical spherical cores, each with radius r separated by a distance $2R$. If we further assume that the cores have rotation periods equal to the orbital period, we obtain a ratio of rotational angular momentum, of the two cores combined $J_{\rm ROT}$, to J_T of

$$\frac{J_{\rm ROT}}{J_T} = \left[1 + \frac{5(R/r)^2}{2}\right]^{-1}. \quad (1)$$

If $r = \frac{1}{2}R$, each core has a rotational angular momentum of only 5% of J_T but has half the total mass, implying an order of magnitude reduction in the angular momentum that can affect further collapse.

It is clear that if the initial angular momentum of molecular clouds is a serious impediment to their collapse, the fragmentation into massive cores will play a major role in the formation of stars. If the velocity differences between adjacent cores do not reflect orbital motion, it is necessary to explain how such massive objects with different velocities could have coalesced or fragmented in such close proximity. Any theory of the evolution of clouds leading to the formation of OB stars must take into account the presence of these 10^2–10^3 $M_\odot$ dense cores, their dynamics, and the tendency of young stars to be at their centers.

We thank W. Glaccum, R. F. Loewenstein, G. Novak, R. Pernic, T. Roelling, and M. Werner for help with the observations, R. Genzel for helpful comments, and M. Werner for providing us his W3 results in numerical form. This work was supported in part by NASA grant NSG 2057 and NSF grant AST-8117134 to the University of Chicago and by NASA grant NAG 2-200 to the University of California. J. A. D. thanks Zonta International for support from an Amelia Earhart Graduate Fellowship.

REFERENCES

Beichman, C. A., Becklin, E. E., and Wynn-Williams, C. G. 1983, *Ap. J. (Letters)*, **232**, L47.
Brackmann, E., and Scoville, N. Z. 1980, *Ap. J.*, **242**, 112.
Cheung, L., Frogel, J. A., Gezari, D. Y., and Hauser, M. G. 1978, *Ap. J. (Letters)*, **226**, L149.
Davidson, J. A., and Jaffe, D. T. 1984, *Ap. J. (Letters)*, **277**, L13.
Dickman, R. L. 1978, *Ap. J. Suppl.*, **37**, 407.
Downes, D., Genzel, R., Becklin, E. E., and Wynn-Williams, C. G. 1981, *Ap. J.*, **244**, 869.
Evans, N. J. II, Blair, G. N., and Beckwith, S. 1977, *Ap. J.*, **217**, 448.
Genzel, R., and Downes, D. 1977, *Astr. Ap. Suppl.*, **30**, 145.
Genzel, R., Downes, D., Ho, P. T. P., and Bieging, J. 1982, *Ap. J. (Letters)*, **259**, L103.
Gezari, D. Y. 1982, *Ap. J. (Letters)*, **259**, L29.
Harper, D. A., Glaccum, W., Loewenstein, R. F., and Pernic, R. 1984, in preparation.
Hildebrand, R. H. 1983, *Q. J.R.A.S.*, **24**, 267.
Ho, P. T. P., Genzel, R., and Das, A. 1983, *Ap. J.*, **266**, 596.
Ho, P. T. P., Martin, R. N., and Barrett, A. H. 1981, *Ap. J.*, **246**, 761.
Howell, R. R., McCarthy, D. W., and Low, F. J. 1981, *Ap. J. (Letters)*, **251**, L21.
Israel, F. P. 1976, *Astr. Ap.*, **52**, 175.
Jaffe, D. T., Hildebrand, R. H., Keene, J., Harper, D. A., Loewenstein, R. F., and Moran, J. M. 1984, *Ap. J.*, **281**, 225.
Jaffe, D. T., Hildebrand, R. H., Keene, J., and Whitcomb, S. E. 1983, *Ap. J. (Letters)*, **273**, L89.
Keene, J., Hildebrand, R. H., and Whitcomb, S. E. 1982, *Ap. J. (Letters)*, **252**, L11.
Lo, K. Y., and Burke, B. F. 1973, *Astr. Ap.*, **26**, 487.
Panagia, N. 1973, *A.J.*, **78**, 929.
Pipher, J. L., and Soifer, B. T. 1976, *Astr. Ap.*, **46**, 153.
Werner, M. W., *et al.* 1980, *Ap. J.*, **242**, 601.
Werner, M. W., Gatley, I., Harper, D. A., Becklin, E. E., Loewenstein, R. F., Telesco, C. M., and Thronson, H. A. 1976, *Ap. J.*, **204**, 420.
Whitcomb, S. E., Hildebrand, R. H., and Keene, J. 1980, *Pub. A.S.P.*, **92**, 863.
Whitcomb, S. E., *et al.* 1984, in preparation.
Wright, E. L., and Odenwald, S. 1980, *Bull. A.A.S.*, **13**, 456.
Wynn-Williams, C. G., Becklin, E. E., Downes, D., and Genzel, R. 1984, *Ap. J.*, **281**, 172.
Wynn-Williams, C. G., Becklin, E. E., and Neugebauer, G. 1972, *M.N.R.A.S.*, **160**, 1.
Ziurys, L. M., Martin, R. N., Pauls, T. A., and Wilson, T. L. 1981, *Astr. Ap.*, **104**, 288.

J. A. DAVIDSON, M. DRAGOVAN, and R. H. HILDEBRAND: Enrico Fermi Institute, University of Chicago, 5640 Ellis Avenue, Chicago, IL 60637

D. T. JAFFE: Space Sciences Laboratory, University of California, Berkeley, CA 94720